Electronic Transactions on Numerical Analysis.
Volume 55, pp. 671–686, 2022.

ISSN 1068–9613.
DOI: 10.1553/etna_vol55s671

ETNA
Kent State University and
Johann Radon Institute (RICAM)

CONSTRUCTING DIFFEOMORPHISMS BETWEEN SIMPLY CONNECTED PLANE DOMAINS*

KENDALL ATKINSON†, DAVID CHIEN‡, AND OLAF HANSEN‡

Abstract. Consider a simply connected domain $\Omega \subset \mathbb{R}^2$ with boundary $\partial\Omega$ that is given by a smooth function $\varphi : [a, b] \mapsto \mathbb{R}^2$. Our goal is to calculate a diffeomorphism $\Phi : \mathbb{B}_1(0) \mapsto \Omega$, $\mathbb{B}_1(0)$ the open unit disk in $\mathbb{R}^2$. We present two different methods where both methods are able to handle boundaries $\partial\Omega$ that are not star-shaped. The first method is based on an optimization algorithm that optimizes the curvature of the boundary, and the second method is based on the physical principle of minimizing a potential energy. Both methods construct first a homotopy between the boundary $\partial\mathbb{B}_1(0)$ and $\partial\Omega$ and then extend the boundary homotopy to the inside of the domains. Numerical examples show that the method is applicable to a wide variety of domains Ω.

Key words. domain transformations, constructing diffeomophisms, shape blending

AMS subject classifications. 65D05, 49Q10

1. Introduction.

Consider being given a boundary curve Γ for a simply connected region Ω in the plane $\mathbb{R}^2$. This is usually given as a function $\varphi : [a, b] \to \mathbb{R}^2$ for some interval $[a, b]$. We want to create a 1-1 function Φ from the unit disk $\mathbb{B}^2$ onto $\overline{\Omega}$ with $\Phi|_\Gamma \equiv \varphi$. In addition, we want to approximate the first derivatives of Φ and its Jacobian. The curve Γ is assumed to be smooth, with $\varphi \in C^2\,[a, b]$, and it is further assumed that φ, φ', φ'' can be computed explicitly.

Creating Φ is a several-step process. We begin by finding the arc length parametrization of Γ. For a given n, an equal subdivision of Γ into n subintervals of equal arc length is created. From it, we create a cubic spline interpolant of Γ, using the nodes associated with the n subdivisions of Γ. This is discussed in Section 2. We then vary this spline function to reduce its variation from a circle of the same arc length. We propose two different approaches to do this, to be discussed in Sections 3 and 4. These methods produce a sequence of boundaries, starting with Γ and going to a circle C of equal arc length. Using the reverse sequence of these boundaries, a mapping from the unit disk is created by solving a suitable differential equation; cf. Section 5.

This problem was explored earlier in [1, Chapter 3] and [2], but it was restricted mainly to regions Ω that are starlike with respect to some point in the region. Methods based on interpolation of the boundary function φ were studied. In addition, an iterative method was introduced to improve the choices of Φ. The methods proposed in this paper can also be used for regions that are not starlike. For other papers concerned with this problem, see [9, 10, 11]. In [4] the optimization of geometries with respect to certain criteria are discussed. This is kind of an opposite problem to the one presented here as the final shape (a circle) is known, but still a transformation has to be constructed.

In the book [1], boundary value problems for partial differential equations are solved over regions that can be transformed to a unit disk. This requires being able to carry out such a transformation, and the present paper shows how to do this. In a further article, the ideas of this paper will be applied to the solution of partial differential equations.

*Received March 19, 2022. Accepted June 23, 2022. Published online on August 22, 2022. Recommended by Tom DeLillo.
†University of Iowa (kendall-atkinson@uiowa.edu).
‡California State University San Marcos ({chien,ohansen}@csusm.edu).

ETNA
Kent State University and
Johann Radon Institute (RICAM)

2. Boundary preliminaries. Let the boundary Γ be given by $\varphi \in C[a,b]$. To calculate its circumference, apply numerical integration to

$$L \equiv \int_a^b |\varphi'(u)|\, du. \tag{2.1}$$

The trapezoidal rule is a logical choice because of the periodicity of the integrand over the interval $[a,b]$.

Let σ denote the arc length as a function of the given parametrization variable τ:

$$\sigma(\tau) \equiv \int_a^\tau |\varphi'(u)|\, du, \qquad a \le \tau \le b.$$

Let $\psi \in C^2[0,L]$ denote the inverse of σ. It satisfies

$$t = \sigma(\psi(t)) = \int_a^{\psi(t)} |\varphi'(u)|\, du, \qquad 0 \le t \le L.$$

Differentiating yields

$$1 = |\varphi'(\psi(t))|\psi'(t).$$

Thus, $\psi(t)$ is the solution of the initial value problem

$$\psi'(t) = \frac{1}{|\varphi'(\psi(t))|}, \qquad 0 \le t \le L,$$

with $\psi(0) = 0$. An ode solver (say `ode113` or `rfk45` within MATLAB) is used to evaluate the solution at n evenly spaced points, with $h = L/n$ the arc length between adjacent evenly spaced nodes. Denote these nodes by $x_0, x_1, \ldots, x_n$, with $x_n = x_0$, and let $\{t_0, t_1, \ldots, t_n\}$ denote the corresponding arc lengths of the nodes from x_0. These are extended periodically, e.g., $x_j = x_{j\pm n}$, and let $\{t_j\}$ also be extended periodically, e.g., $t_{j\pm n} = t_j \pm L$.

We replace the parametrization of Γ with a periodic cubic spline that interpolates Γ at the nodes. Denote this cubic spline by $\eta \in C_p^2[0,L]$, a periodic C^2-function on $(-\infty,\infty)$ with

$$\eta(t_i) = x_i, \qquad i = 0, 1, \ldots, n.$$

The equal spacing of the arc length parameters $\{t_i\}$ leads to a simple representation for η.

Introduce the cubic B-spline

$$B(u) = \frac{1}{6}\Big\{(4-u)_+^3 - 4(3-u)_+^3 + 6(2-u)_+^3 - 4(1-u)_+^3 + (0-u)_+^3\Big\},$$

where

$$(y)_+^3 = \begin{cases} y^3, & y \ge 0, \\ 0, & y < 0. \end{cases}$$

See Figure 2.1. The support of $B(t)$ is $(0,4)$. Introduce

$$B(x,j;h) = B((x-t_j)/h), \qquad -\infty < x < \infty, \quad j = 0, \pm 1, \pm 2, \ldots$$

The support of $B(x,j,h)$ is (t_j, t_{j+4}).

ETNA
Kent State University and
Johann Radon Institute (RICAM)

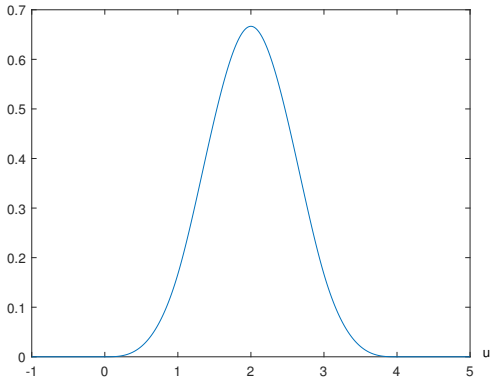

FIG. 2.1. *Graph of* $B(u)$.

We want a function

$$p(x) = \sum_{j=-\infty}^{\infty} \alpha_j B(x, j; h). \tag{2.2}$$

To make this periodic with period $L = nh$, we make the coefficients $\alpha_j \in \mathbb{R}^2$ periodic in j with period n,

$$\alpha_{j+n} = \alpha_j, \qquad j = 0, \pm 1, \pm 2, \ldots$$

Consider interpolation of a periodic function $f(t)$ at the nodes $\{t_j\}$, with L an integer multiple of the period of f. For this we must solve the linear system

$$\sum_{j=-\infty}^{\infty} \alpha_j B(t_i, j; h) = f(t_i), \qquad i = 0, \pm 1, \pm 2, \ldots \tag{2.3}$$

We need to consider only the case of $i = 1, \ldots, n$ because of periodicity. The resulting linear system for $\{\alpha_1, \ldots, \alpha_n\}$ is diagonally dominant with diagonal elements $\frac{2}{3}$ and the off-diagonal elements in each equation summing up to $\frac{1}{3}$. The matrix of coefficients is

$$\frac{1}{6}\begin{bmatrix} 4 & 1 & 0 & \cdots & & 0 & 1 \\ 1 & 4 & 1 & 0 & \cdots & & 0 \\ 0 & 1 & 4 & 1 & 0 & \cdots & 0 \\ \vdots & & & \ddots & & & \\ & & & & \ddots & & \\ 0 & \cdots & & 0 & 1 & 4 & 1 \\ 1 & 0 & \cdots & & 0 & 1 & 4 \end{bmatrix}.$$

This proves the existence of a unique solution $p(x; h)$ to the interpolation problem, and it will be periodic. It will also be a cubic spline function with knots $\{t_0, t_1, \ldots, t_n\}$. The cost of solving the system (2.3) is $\mathcal{O}(n)$. This spline interpolation is applied to both components of the parametrization $\varphi(\psi(t))$, $0 \le t \le L$.

ETNA
Kent State University and
Johann Radon Institute (RICAM)

3. Moving toward a circle by using optimization. Before we discuss two different methods to connect the boundary Γ to a circle C with the same arc length in the current and following section, we like to remark why we did not choose to use the 'obvious' way of connecting the two curves. By the obvious way we denote the following homotopy: Assume that $p(x)$, $x \in [0, L]$, is an arc length parametrization of Γ and $q(x)$, $x \in [0, L]$, is an arc length parametrization of the circle C. Then one can define the homotopy $H(t, x)$, $(t, x) \in [0, 1] \times [0, L]$, by

$$H(t, x) = (1 - t)p(x) + tq(x).$$

It turns out that this approach has two problems. First, it is not clear that the intermediate curves $H(t, \cdot)$, $0 < t < 1$, are simple closed curves that enclose an open domain. Second, when we used this transformation to construct a mapping of the disk to Ω, the resulting mappings for the enclosed region (see Section 5) seem to show a wide variation of the Jacobian. Therefore we looked at alternative methods to map C to Γ, and two methods that we discovered are presented below.

Consider perturbing the coefficients in (2.2), producing a new spline formula:

$$p(x; \delta) = \sum_{j=-\infty}^{\infty} (\alpha_j + \delta_j) B(x, j; h), \tag{3.1}$$

with the $\delta_j \in \mathbb{R}^2$ periodic in j with period n. Proceed by making the curvature closer to that of a circle with circumference L, which has constant curvature

$$\frac{2\pi}{L}. \tag{3.2}$$

Calculate the curvature of the modified curve at each x_j as

$$\kappa(x_j; \delta) = \frac{p'(x_j; \delta)_1 p''(x_j; \delta)_2 - p'(x_j; \delta)_2 p''(x_j; \delta)_1}{(p'(x_j; \delta)_1^2 + p'(x_j; \delta)_2^2)^{3/2}}.$$

Note the use of subscripts for the 2-vector $p(x; \delta)$. The distance between nodes is maintained by requiring

$$|p(x_{j-1}; \delta_{j-1}) - p(x_j; \delta_j)| = h, \qquad j = 1, \ldots, n. \tag{3.3}$$

This places n constraints on the $2n$ real variables $\{\delta_j\}$. To restrict the growth of δ, size restrictions are placed on $\{\delta_1, \ldots, \delta_n\}$,

$$|\delta_j| \le A, \qquad j = 1, \ldots, n, \tag{3.4}$$

for some $A > 0$. Finally, the restriction

$$\delta_0 = 0 \tag{3.5}$$

is used to fix the curve with respect to the node x_0.

To make the curvature closer to that of (3.2), introduce the function

$$f(\delta) = \sqrt{\sum_{j=1}^{n} w_j \left(\kappa(x_j; \delta) - \frac{2\pi}{L} \right)^2} \tag{3.6}$$

ETNA
Kent State University and
Johann Radon Institute (RICAM)

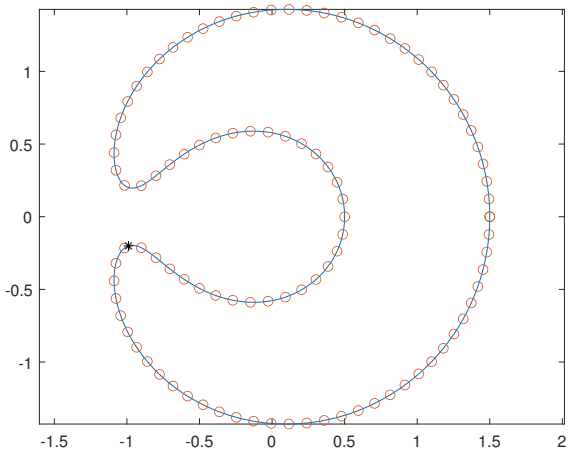

FIG. 3.1. *Pacman $\varphi(u)$ over $[0, 2\pi]$. '*' indicates the maximum curvature.*

with $\{w_j\}$ positive weights summing up to 1. We use both equal weights and weights proportional to the curvature of the original curve Γ. The choice of δ in (3.1) comes from optimizing $f(\delta)$ subject to the constraints (3.3)–(3.5). In our examples, we have used `fmincon` from the MATLAB optimization library. For the weights $\{w_j\}$, we alternate between equal weights and weights proportional to the absolute value of the curvature on the original curve at the nodes $\{x_j\}$. This alternation has led experimentally to a more robust iteration. Using just one choice of $\{w_j\}$ also converges, although not as rapidly.

As will be explained further in Section 5, we need a sequence of changes in Γ with an 'easy change' from each member of the sequence to the next element of the sequence. We control this in part by our choice of the constant A in (3.4). However, too small a choice for A often slows the iteration a great deal.

EXAMPLE 3.1. Consider the 'Pacman' boundary given by

$$\varphi(u) = (1 + a\cos(u)) \begin{bmatrix} \cos(f \sin u) \\ \sin(f \sin u) \end{bmatrix}, \qquad 0 \le u \le 2\pi,$$

with $a = 0.5$ and $f = \pi - 0.2$. It is illustrated in Figure 3.1 with $n = 100$ nodes created using subdivisions according to arc length, indicated by $\circ$. The curvature with respect to arc length is shown in Figure 3.2. The arc length (2.1) was approximated using the trapezoidal rule with $m = 300$ subdivisions; the arc length is approximately $L \doteq 12.2356817$. The maximum deviation of the interpolatory spline from the true curve was 0.00463, although it was much less at most points. The deviation was greatest at the points of maximum curvature. The region interior to Γ is not starlike with respect to any point, and therefore the ideas in [2] are not applicable.

Apply the optimization method associated with (3.3)–(3.6), and use $A = 1.0$ for the bound for the perturbations in δ. The iterates are shown in Figure 3.3. The equally spaced points on the final circle are marked by $\circ$. The iterations have the repeating pattern of red, green, and blue. The final iterate is a circle of approximate radius

$$R = \frac{L}{2\pi} \doteq \frac{12.2356817}{2\pi} \doteq 1.94737.$$

The curvature of the final circle should be $1/R \doteq 0.51351$, and the curvature of the final circular curve in Figure 3.3 varies over $[0.5125, 0.5145]$.

ETNA
Kent State University and
Johann Radon Institute (RICAM)

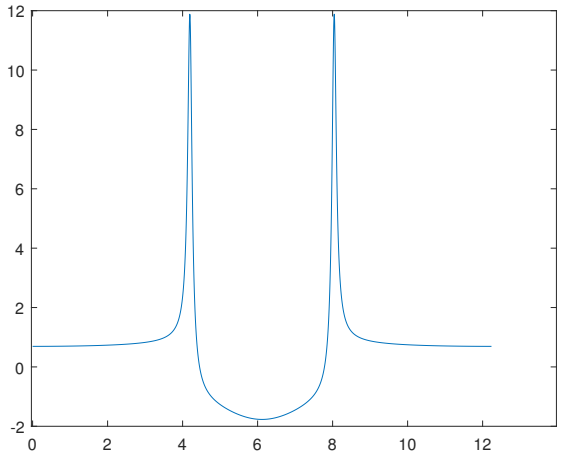

FIG. 3.2. *Curvature of Pacman curve.*

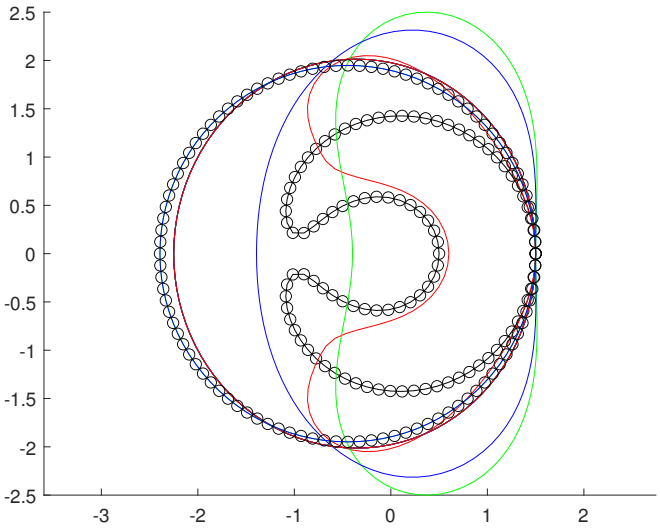

FIG. 3.3. *Iterations for Pacman curve.*

EXAMPLE 3.2. Consider the boundary Γ given by

$$\varphi(u) = \begin{bmatrix} (5 + \sin u - 1.5\sin(3u) - \cos(5u))\cos u \\ (5 + \sin u + \sin(3u) - 3\cos(5u))\sin u \end{bmatrix}, \qquad 0 \le u \le 2\pi. \tag{3.7}$$

It is displayed in Figure 3.4 with $n = 100$ nodes created using subdivisions according to arc length, indicated by $\circ$. It will be referred to as an amoeba boundary. The arc length (2.1) was approximated using the trapezoidal rule with $m = 300$ subdivisions; the arc length is approximately $L \doteq 57.253363$. The curvature with respect to arc length is shown in Figure 3.5. The maximum deviation of the interpolatory spline from the true curve was 0.063, although it was much less at most points. The deviation was greatest at the points of maximum curvature.

ETNA
Kent State University and
Johann Radon Institute (RICAM)

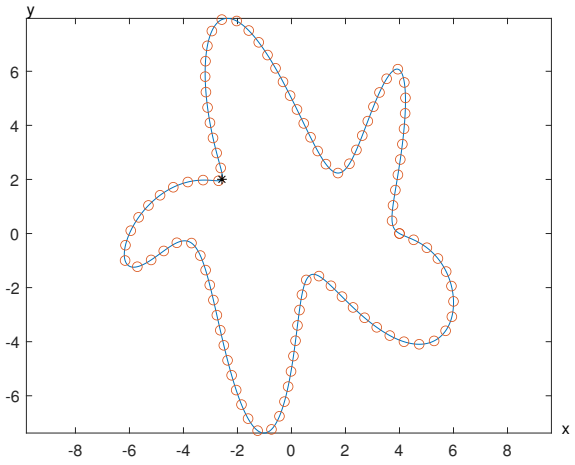

FIG. 3.4. *Amoeba $\varphi(u)$ over $[0, 2\pi]$. '*' indicates the maximum curvature.*

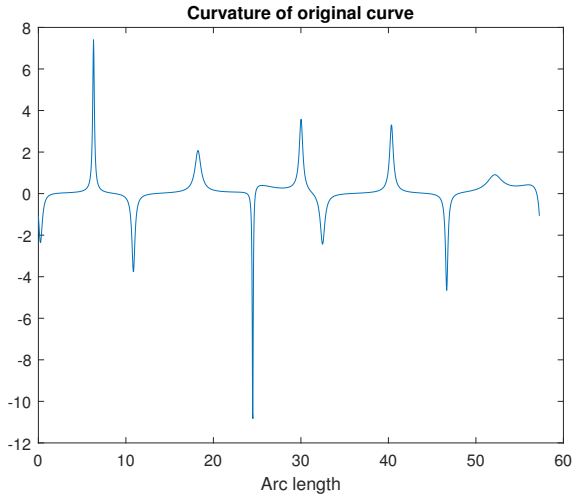

FIG. 3.5. *Curvature of (3.7) with respect to arc length.*

The region interior to Γ is not starlike with respect to any point, and therefore the ideas in [2] are not applicable.

Apply the optimization method associated with (3.3)–(3.6). Equal weights $\{w_j\}$ are used in (3.6). Use $A = 2.0$ for the bound for the perturbations in δ and $n = 100$. The iterates are presented in Figure 3.6. The iterations have the repeating pattern of red, green, and blue. The final iterate is a circle of approximate radius

$$R = \frac{L}{2\pi} \doteq \frac{57.253363}{2\pi} \doteq 9.11216.$$

The curvature of the final circle should be $1/R \doteq 0.109744$, and the curvature of the final circular curve in Figure 3.6 varies over $[0.10960, 0.10983]$.

ETNA
Kent State University and
Johann Radon Institute (RICAM)

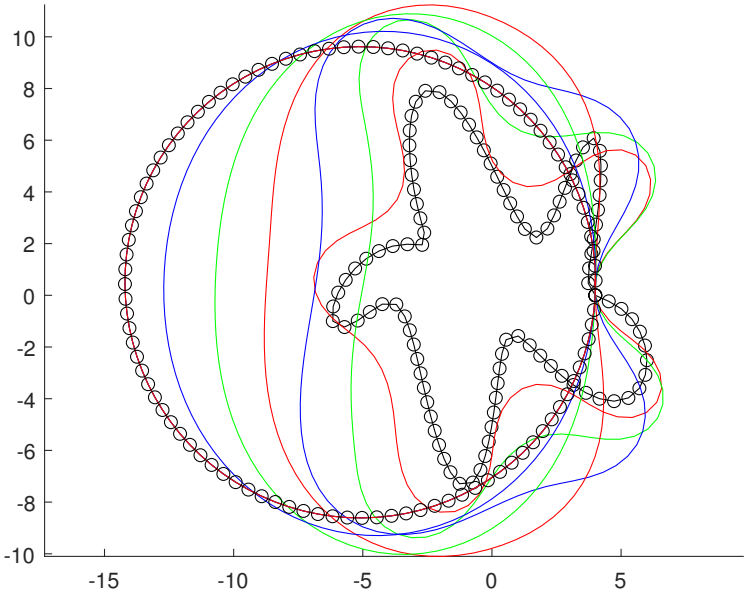

FIG. 3.6. *Iterations due to minimizing (3.6).*

4. Moving toward a circle by minimizing energy. As in the previous Section 3, we assume that the boundary Γ is given by a function $p(x)$ (see (2.2)) and that $0 \le x \le L$ is the arc length parameter. So the points $p_i = p(iL/n)$ have an approximately equal spacing

$$|p_i - p_{i+1}| \approx \frac{L}{n}.$$

In practice this condition is better satisfied if n is increased, but we will assume

$$|p_i - p_{i+1}| = \frac{L}{n} \equiv \Delta$$

in the following to simplify the presentation of the algorithm. Figure 3.1 displays an example of the Pacman boundary Γ and p_i, $i = 1, \ldots, 100$.

The idea for our algorithm comes from a physical experiment. Assume that we have a flexible closed conductor loop in the shape of Γ that is charged sufficiently high. Then the loop will unfold and take the shape of a circle to minimize the potential energy. A discrete version of this experiment is that we have metallic pearls attached equidistantly along a string in the shape of Γ and the pearls all carry the same electrical charge. We call these pearls charges in the following. The connection between two charges is rigid, so the distance between the charges is fixed. If the charges can move and the charge is sufficiently high, then they will move into the positions of a regular n-gon to minimize the energy.

The differential algebraic equation (DAE) for this situation is the following:

$$p_i''(t) = \sum_{j=1,\, j\neq i}^{n} \frac{1}{|p_i(t) - p_j(t)|^3} \left(p_i(t) - p_j(t)\right), \qquad i = 1, \ldots, n,\ t > 0, \tag{4.1}$$

$$\Delta^2 = \begin{cases} |p_i - p_{i+1}|^2, & i = 1, \ldots, n-1, \\ |p_n - p_1|^2. \end{cases} \tag{4.2}$$

ETNA
Kent State University and
Johann Radon Institute (RICAM)

Here we assume that the position p_i of the charge i depends on time $t \geq 0$, and we have set all physical constants equal to 1. The initial conditions $p_i(0)$ are given by their initial position along Γ, as in the above Figure 3.1.

There are two problems with the above formulation. First, equation (4.1) conserves energy, so if the charges p_i move towards their position along the regular n-gon, they have an excess of kinetic energy and will be oscillating around their position in the n-gon. To remove energy from the above system we will include a friction term defined by a constant $\alpha > 0$ that will determine how fast the charges will loose their kinetic energy.

Second, the final position of the n-gon is determined by the differential equation (4.1), but once the charges are in the final position, the energy is not changed if we move the n-gon or rotate it. Numerically we will need to ensure (4.2) by using Newton's method. Our numerical experiments showed that eliminating these two degrees of freedom (straight movement and rotation) simplifies the numerical implementation. We remove these two degrees of freedom by fixing the positions of $p_1(t)$ (no straight movements anymore) and $p_n(t)$ (no rotational freedom anymore). Instead of p_1 and p_n we could have chosen any other neighboring pair of charges.

These two modifications lead to our final DAE

$$p_i''(t) = \sum_{j=1,\, j\neq i}^{n} \frac{1}{|p_i(t) - p_j(t)|^3} \left(p_i(t) - p_j(t)\right) - \alpha p_i'(t), \quad i = 2, \ldots, n-1,\ t > 0, \tag{4.3}$$
$$\Delta^2 = |p_i - p_{i+1}|^2, \qquad i = 1, \ldots, n-1.$$

To simplify the notation we introduce a vector of all movable charge positions (from now on we consider p_1 and p_n as constants):

$$P(t) = (p_2(t), \ldots, p_{n-1}(t))^T \in \mathbb{R}^{2(n-2)}$$

and the function

$$g(P(t)) = \big(|p_1 - p_2(t)|^2 - \Delta^2, |p_2(t) - p_3(t)|^2 - \Delta^2, \ldots,$$
$$\ldots, |p_{n-1}(t) - p_n|^2 - \Delta^2\big)^T \in \mathbb{R}^{n-1}.$$

Now the above differential algebraic system can be written as

$$P''(t) = F(P(t), P'(t)), \quad t > 0,$$
$$g(P(t)) = 0 \qquad\qquad \in \mathbb{R}^{n-1},$$

with initial condition $P(0) = P_0 = (p_2, \ldots, p_{n-1})$ and F defined according to (4.3).

We use an Euler-Lagrange formulation (see [7, VI.5]) and add constraint forces that will enforce $g(P(t)) = 0$:

$$P''(t) = F(P(t), P'(t)) - G^T(P(t))\lambda(t), \quad t > 0,$$
$$g(P(t)) = 0 \qquad\qquad\qquad\qquad \in \mathbb{R}^{n-1},$$

where $G(P(t)) = \left(\frac{\partial g_i(P(t))}{\partial p_j}\right)_{i,j}$ is the Jacobi matrix and $\lambda = (\lambda_1(t), \ldots, \lambda_{n-1}(t))$ are Lagrange multipliers.

Lastly, we transform the above system into a system of order 1 by introducing the velocity vector $Q(t)$:

$$Q(t) = P'(t).$$

ETNA
Kent State University and
Johann Radon Institute (RICAM)

Then the above second-order differential algebraic system can be written as

$$P'(t) = Q(t), \tag{4.4}$$

$$Q'(t) = F(P(t), Q(t)) - G^T(P(t))\lambda(t), \qquad t > 0, \tag{4.5}$$

$$g(P(t)) = 0.$$

This is a DAE of index 3; see [7]. Before we start to solve this equation numerically, there are two questions: What value we use for α and on which time interval $[0, T]$ we solve the DAE (4.4), (4.5).

In our experiments we found that a range of $\alpha \in [1, 20]$ leads to a fast convergence of $P(t)$ to a regular n-gon. In general a larger α means it takes longer to reach the n-gon position, but a larger α also leads to a smoother movement of the charges towards their final position.

To determine T we monitor how far away from a circle the charges $P(t)$ are. Once we find a circle such that all points in $P(t)$ are within $\varepsilon > 0$ of the circle, we stop the time integration. In our experiments we use $\varepsilon = 0.01$. We have implemented this in the following way: Given a set of points p_i, $i = 1, \ldots, n$, we calculate the center

$$C = \frac{1}{n} \sum_{i=1}^{n} p_i$$

of the points and an average radius

$$R = \frac{1}{n} \sum_{i=1}^{n} |p_i - C|.$$

We stop the time integration once

$$\max_{i=1}^{n} \big| |p_i - C| - R \big| \leq \varepsilon.$$

To solve the DAE (4.4), (4.5) we use a backward difference method (BDF of order 2; see [6, III.6]) with a Newton method to solve the nonlinear equation system in each step. The step length is variable such that the estimated local integration error is smaller than a given tolerance τ, $\tau = 0.001$ in our experiments. At the end of the numerical integration we have a sequence $\widetilde{P}(t_i)$, $i = 0, \ldots, N_T$, $t_0 = 0$, $t_{N_T} = T$.

Then we get a numerical approximation $\widetilde{P}(t)$, $t \in [0, T]$, for $P(t)$. Here we can use again spline interpolation or piecewise linear interpolation to extend $\widetilde{P}(t_i)$ to the interval $[0, T]$. As in Section 3, the final movement from the circle $\widetilde{P}(T)$ to Γ that corresponds to $\widetilde{P}(0)$ is given by time reversal $\widetilde{P}(T - t)$, $t \in [0, T]$.

Figures 4.1 and 4.2 display the trajectories of $\widetilde{P}(t)$ that move the points from Γ in Figure 3.1 to a circle C; here the friction parameters are $\alpha = 5$ in Figure 4.1 and $\alpha = 15$ in Figure 4.2. For a fixed t, $0 < t < T$, we have a sequence of points in $\widetilde{P}(T - t)$ that represent an intermediate curve between a circle, $t = 0$, and Γ, $t = T$. By using spline interpolation we can expand the points at $T - t$ to a continuous curve. Together with the above mentioned interpolation in time we have found a homotopy between a circle and Γ, which we will denote by

$$H(t, x), (t, x) \in [0, T] \times [0, L],$$

where for a constant iL/n, $H(\cdot, iL/n)$ is given by, for example, piecewise linear interpolation in time of the values of $\widetilde{P}(t_i)$, and for a fixed t, $H(t, \cdot)$ is given by periodic spline interpolation of the $H(t, iL/n)$, $i = 0, \ldots, n$.

ETNA
Kent State University and
Johann Radon Institute (RICAM)

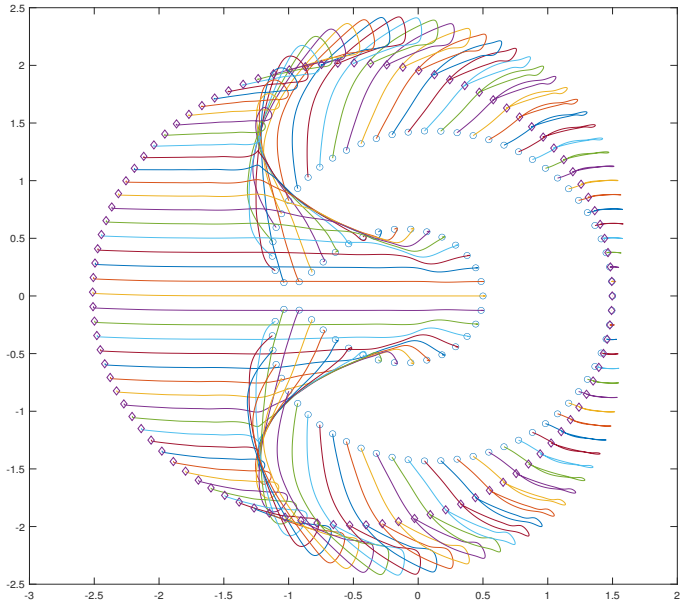

FIG. 4.1. *The trajectories of 100 points moving from the Pacman curve to a circle with friction coefficient* $\alpha = 5$.

The numerical function H depends on n, the discretization of Γ, α, ϵ, and τ, but we will in general not indicate this dependence.

Similar to this section, the optimization method described in Section 3 also leads to a homotopy $H(t,x)$. In the previous Section 3 the optimization function produced a sequence of boundary curves $\widetilde{\Gamma}_0$ to $\widetilde{\Gamma}_N$ (in opposite order). Each curve $\widetilde{\Gamma}_i$ is given by a spline function $p_i(x)$ with arc length parameter $x \in [0, L]$. Remember $\widetilde{\Gamma}_0$ is a circle and $\widetilde{\Gamma}_N = \partial\Omega$. Typically, N is much smaller than the number N_T of the intermediate curves of the current section. By choosing A (see (3.4)) small enough we can assume that all curves $\widetilde{\Gamma}_i$, $i = 1, \ldots, N$, are simple and can be connected without self-intersection. The connecting curves can be, for example, given by straight lines or splines. We introduce an artificial time t, $0 \le t \le N$, and this defines a homotopy

$$\widetilde{H}(t,x), (t,x) \in [0,N] \times [0,L]$$

between $\widetilde{\Gamma}_0$ and $\partial\Omega = \widetilde{\Gamma}_N$. We will denote $\widetilde{H}$ also by H in the following sections and write T instead of N.

In conclusion, we have described two algorithms that lead to a homotopy between a circle C of circumference L and a given curve Γ of length L. These homotopies H will be the foundation for the algorithm in Section 5, where we will construct a mapping between the disk with boundary C and the domain Ω that is bounded by Γ.

5. Mapping the disk to Ω . Following Sections 3 and 4, we now have a homotopy $H(t,x)$ that connects the circle

$$\Gamma_0 = \{H(0,x) \mid 0 \le x \le L\}$$

and $\Gamma = \partial\Omega$, with x denoting arc length. Let $\mathbb{D}$ denote the open disk whose boundary is the circle associated with Γ_0, as obtained in the preceding two sections. It is straightforward to

ETNA
Kent State University and
Johann Radon Institute (RICAM)

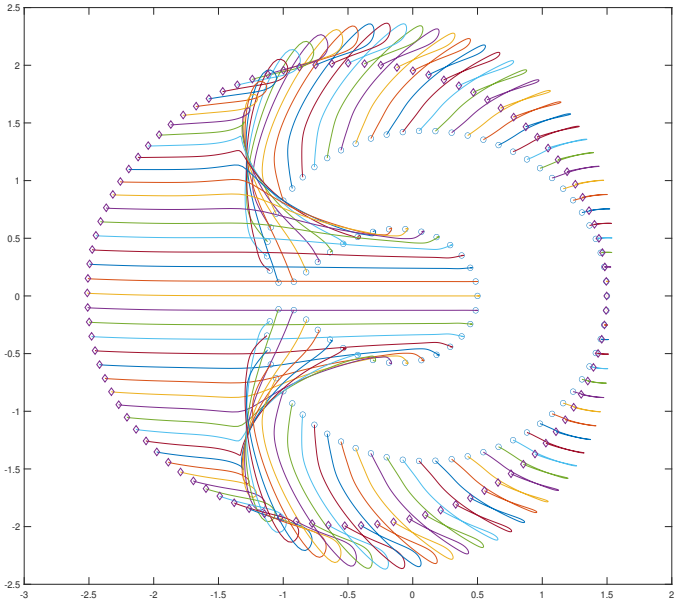

FIG. 4.2. *The trajectories of 100 points moving from the Pacman curve to a circle with friction coefficient* $\alpha = 15$.

map the unit disk $\mathbb{B}^2$ to the disk $\overline{\mathbb{D}}$ with a smooth bijective function Φ_0. So, once we have constructed a smooth bijective function Φ_1 from $\mathbb{D}$ to Ω as a continuous extension of the homotopy H, we have found the desired mapping

$$\Phi : \mathbb{B}^2 \to \overline{\Omega}$$

as the composition $\Phi = \Phi_1 \circ \Phi_0$. The function H defines a sequence of boundary curves

$$\Gamma_t = \{H(t,x) \mid 0 \le x \le L\}, \qquad 0 \le t \le T,$$

with $\Gamma_T = \Gamma = \partial\Omega$. We denote the interior of Γ_t by $\mathbb{D}_t$, so $\mathbb{D}_0 = \mathbb{D}$ and $\mathbb{D}_T = \Omega$.

For a fixed $x \in [0, L]$, the function $\psi(t) = H(t,x)$ defines a trajectory that starts at a point $\mu = H(0,x) \in \Gamma_0$ and ends at a point $\beta = H(T,x) \in \Gamma_T$. The function $\psi(t)$ can be considered the solution of the initial value problem.

$$\begin{aligned} \dot{\psi}(t) &= V(t,\psi(t)), \quad 0 < t \le T, \\ \psi(0) &= \mu \qquad\qquad\quad \in \Gamma_0, \end{aligned}$$

with the vector field

$$V(t,\xi) = \frac{\partial H(t, \mathbf{x}_t(\xi))}{\partial t}$$

given along Γ_t, $t \in [0,T]$. Here $\mathbf{x}_t(\xi)$ is the function that assigns to a $\xi \in \Gamma_t$ the arc length value x with $\xi = H(t,x)$. Figure 4.1 and 4.2 illustrate some of the $\psi(t)$ (for various initial values μ) for the Pacman curve, and Figure 3.3 illustrates a sequence of $\mathbb{D}_t$. To indicate the dependence of $\psi(t)$ on the starting point $\mu = H(0,x)$ we will use the notation $\psi_\mu(t)$ from now on.

ETNA
Kent State University and
Johann Radon Institute (RICAM)

We follow the approach of [5, Section 5, Theorem 5.13] and continuously extend the vector field V to a vector field $\mathcal{V}$ on $\mathbb{D}_t$ by 'k-transfinite barycentric interpolation',

$$\mathcal{V}(t,\xi) = \frac{1}{\int_{\Gamma_t} \frac{1}{|\eta-\xi|^k}\, ds_\eta} \int_{\Gamma_t} \frac{V(t,\eta)}{|\eta-\xi|^k}\, ds_\eta, \qquad \xi \in D_t, \quad 0 \le t \le L, \tag{5.1}$$

where $k > 1$ is a parameter. It is shown in [5] that $\mathcal{V}$ is continuous on $\mathbb{R}^2$ and that $\mathcal{V}(t,\xi) = V(t,\xi)$ for $\xi \in \Gamma_t$; see [5, Theorem 3.5].

This vector field allows us to define trajectories $\psi_\mu(t)$ to all $\mu \in \mathbb{D}_0$ by defining $\psi_\mu(t)$ as the solution of the initial value problem

$$\dot{\psi}_\mu(t) = \mathcal{V}(t, \psi_\mu(t)), \quad 0 < t \le T, \tag{5.2}$$

$$\psi_\mu(0) = \mu \qquad\qquad \in \mathbb{D}_0. \tag{5.3}$$

This defines a smooth mapping $\Phi_1(\mu) = \psi_\mu(T)$ that maps $\mathbb{D}_0$ to $\mathbb{D}_T = \Omega$. By our construction, Φ_1 maps Γ_0 1-1 into $\Gamma = \partial\Omega$ because the solutions to the initial value problems (5.2),(5.3) are unique.

As $\Gamma_T = \partial\Omega$ is the boundary of Ω and

$$H(0,x) \overset{\Phi_1}{\mapsto} H(T,x), \qquad x \in [0,L],$$

maps the boundary of the disk $\mathbb{D}_0$ to the boundary of $\Omega = \mathbb{D}_T$, the mapping degree (see [3]) is $d(\Phi_1, \mathbb{D}_0, y) = 1$ for every $y \in \Omega = \mathbb{D}_T$. So, the mapping $\Phi_1 : \mathbb{D}_0 \mapsto \mathbb{D}_T$ is surjective. This shows that Ψ_1 is a bijective mapping from the closed disk $\overline{\mathbb{D}}_0$ to $\overline{\mathbb{D}}_T = \overline{\Omega}$.

Because our goal is to use the mapping Φ_1 for the solution of boundary value problems on Ω (see [1]) we will also need to approximate the Jacobi matrix $J(\mu) = (J_{i,j}(\mu))_{i,j=1,2}$ with

$$J_{i,j}(\mu) = \frac{\partial \Phi_{1,i}}{\partial x_j}(\mu),$$

where we denote the two components of Φ_1 by $\Phi_{1,1}$ and $\Phi_{1,2}$. The Jacobi matrix $J(\mu)$ is given by $J(\mu) = Y_\mu(T)$. Here $Y_\mu(t)$ is the solution of the initial value problem

$$\dot{Y}_\mu(t) = D\mathcal{V}(t, \psi_\mu(t)) \cdot Y_\mu(t), \qquad 0 < t \le T, \tag{5.4}$$

$$Y_\mu(0) = I_{2,2}, \tag{5.5}$$

with $I_{2,2}$ the identity matrix and $D\mathcal{V}$ the Jacobi matrix of $\mathcal{V}$ that is determined by the derivatives of the boundary integral in (5.1). See [8, Section 3.1] for a derivation of (5.4), (5.5).

To approximate Φ_1 numerically we can integrate the initial value problems (5.2), (5.3) and (5.4), (5.5) simultaneously for a set of points $\mu \in \mathbb{D}_0$. To numerically approximate $\Phi_1(\mu)$ and $J(\mu)$ we can use any method to numerically integrate the initial value problems (5.2), (5.3) and (5.4), (5.5). We have initially used an explicit Euler method and all examples in the following section are generated with the explicit Euler method.

6. Numerical examples. In this last section we illustrate our algorithm by presenting the images of a grid on the unit disk in the corresponding domains Ω.

On the unit disk we consider grids as shown in Figure 6.1. It has 82 radial lines and 11 circumferential lines. For every grid point μ in Figure 6.1 we calculate a numerical approximation $\widetilde{\psi}_{\mu,h,n}$ to the trajectory ψ_μ given by (5.2), (5.3). We have used $k = 2$ in (5.1) that defines the right-hand side of (5.2) for the examples in this section. As mentioned in Section 5, the numerical solutions are calculated by using an explicit Euler method with step

ETNA
Kent State University and
Johann Radon Institute (RICAM)

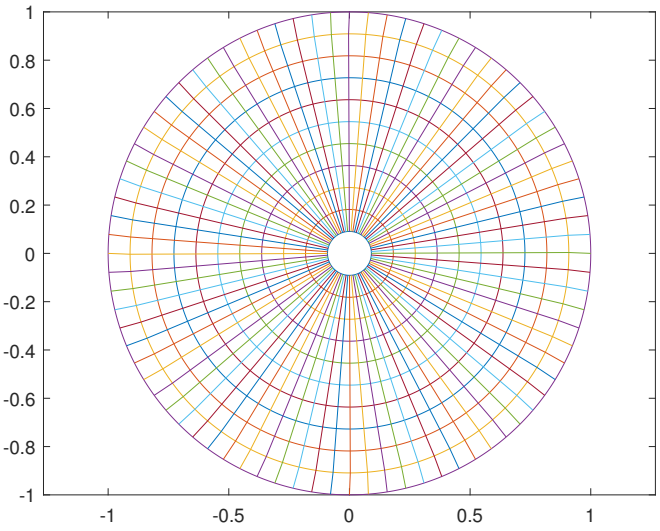

FIG. 6.1. *Grid on the unit disk.*

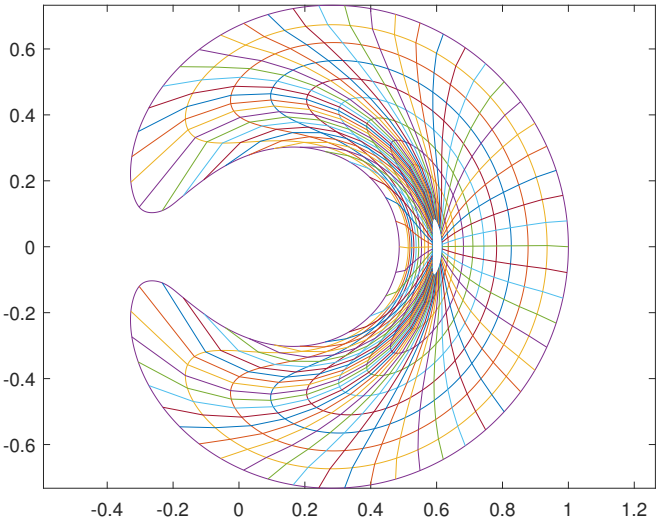

FIG. 6.2. *Grid on Pacman.*

length h. The resulting images of the grid for the two domains shown in Figures 3.1 and 3.4 are given in Figures 6.2 and 6.3. Here the image points $\widetilde{\psi}_{\mu,h,n}(T)$ are connected to mark their position and illustrate the deformation.

The step length h for the calculation of $\widetilde{\psi}_{\mu,h,n}$ was determined experimentally. It was chosen small enough to guarantee that the image of the grids did not overlap. In a similar way, the parameter $n \in \mathbb{N}$ was determined in order to approximate the vector field $\mathcal{V}$ in

ETNA
Kent State University and
Johann Radon Institute (RICAM)

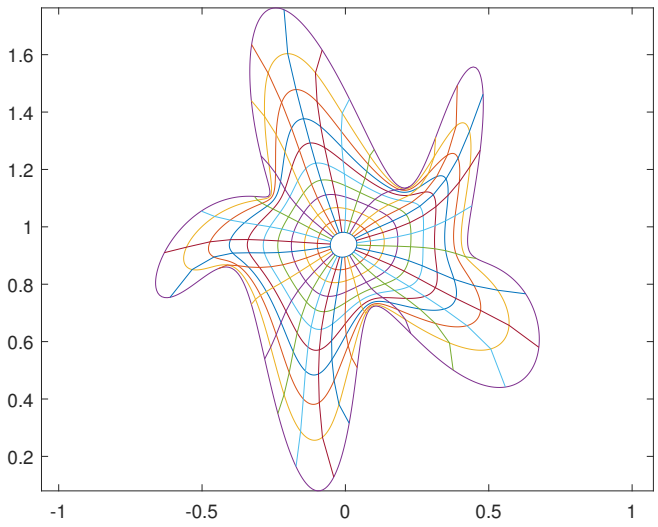

FIG. 6.3. *Grid on amoeba.*

equation (5.2) sufficiently well. We used a trapezoidal rule for both integral terms

$$\mathcal{V}(t,\xi) \approx \mathcal{V}_n(t,\xi) = \frac{1}{\frac{L}{n}\sum_{i=0}^{n-1}\frac{1}{|H(t,iL/n)-\xi|^k}}\,\frac{L}{n}\sum_{i=0}^{n-1}\frac{H(t,iL/n)}{|H(t,iL/n)-\xi|^k}. \tag{6.1}$$

Remember that L is the length of the original boundary Γ of Ω and that the parametrizations $H(t,\cdot)$ are all parametrized with respect to arc length. Formula (6.1) implies that the numerical trajectory $\widetilde{\psi}_{\mu,h,n}$ is the result of applying the explicit Euler method to the initial value problem

$$\begin{aligned}
\dot{\psi}_\mu(t) &= \frac{\sum_{i=0}^{n-1}\frac{H(t,iL/n)}{|H(t,iL/n)-\psi_\mu(t)|^k}}{\sum_{i=0}^{n-1}\frac{1}{|H(t,iL/n)-\psi_\mu(t)|^k}}, && 0 < t \le T,\\
\psi_\mu(0) &= \mu && \in \mathbb{D}_0.
\end{aligned}$$

Note that on a computer with parallel processors, these equations can be solved independently for different choices of grid points μ.

For the application of our method to the solution of boundary value problems on Ω we will need to investigate the accuracy of $\widetilde{\psi}_{\mu,h,n}$ as a function of h and n further. In [1, Section 4.1] we analyzed the influence of the mapping functions ψ on the performance (convergence and condition number) of spectral methods. The methods of the current paper allow us to find additional mapping functions for more complex domains than we could handle in our previous work [2, 1]. This will be the subject of a forthcoming paper.

Our methods can be used to generate grids, as is illustrated in Figures 6.2 and 6.3. But the resulting grids may not be of practical use because of the sometimes odd shape of cells in the grid. The main use to which we are putting our mapping ideas is to carry out the numerical methods in [1], where an explicit differentiable mapping of the unit disk onto the region Ω is needed.

ETNA
Kent State University and
Johann Radon Institute (RICAM)

REFERENCES

[1] K. ATKINSON, D. CHIEN, AND O. HANSEN, *Spectral Methods Using Multivariate Polynomials On The Unit Ball*, CRC Press, Boca Raton, 2019.
[2] K. ATKINSON AND O. HANSEN, *Creating domain mappings*, Electron. Trans. Numer. Anal., 39 (2012), pp. 202–230.
http://etna.ricam.oeaw.ac.at/vol.39.2012/pp202-230.dir/pp202-230.pdf
[3] K. DEIMLING, *Nonlinear Functional Analysis*, Springer, Berlin, 1985.
[4] M.C. DELFOUR AND J.-P. ZOLÉSIO, *Shapes and Geometries*, SIAM, Philadelphia, 2011.
[5] M.C. DELFOUR AND A. GARON, *Transfinite interpolations for free and moving boundary problems*, Pure Appl. Funct. Anal., 4 (2019), pp. 765–801.
[6] E. HAIRER, S.P. NØRSETT, AND G. WANNER, *Solving Ordinary Differential Equations I*, Springer, Berlin, 1987.
[7] E. HAIRER AND G. WANNER, *Solving Ordinary Differential Equations II*, Springer, Berlin, 1991.
[8] E. HILLE, *Lecture on Ordinary Differential Equations*, Addison-Wesley, Reading, 1969.
[9] M. SABA, T. SCHNEIDER, K. HORMANN, AND R. SCATENI, *Curvature-based blending of closed planar curves*, Graph. Models, 76 (2014), pp. 263–272.
[10] T. W. SEDERBERG, P. GAO, G. WANG, AND H. MU, *2-D shape blending: an intrinsic solution to the vertex path problem*, in SIGGRAPH '93: Proceedings of the 20th Annual Conference on Computer Graphics and Interactive Technique, ACM, New York, 1993, pp. 15–18.
[11] T. SURAZHSKY AND G. ELBER, *Metamorphosis of planar parametric curves via curvature interpolation*, Int. J. Shape Model., 8 (2002), pp. 201–216.